ARTICLE

Theoretical studies on the initial reaction kinetics and mechanisms of p-, m- and o-nitrotoluene

Meng Yang,[a] Caiyue Liao,[a] Chenglong Tang,[a,*] Peng Zhang,[b] and Zuohua Huang[a]

The potential energy surfaces (PES) of three nitrotoluene isomers, i.e., p-nitrotoluene, m-nitrotoluene and o-nitrotoluene have been built by CCSD(T)/CBS method. The geometries of reactants, transition states (TS) and products are optimized at B3LYP/6-311++G(d,p) level. Results show that reactions of -NO_2 isomerizing to ONO, and C-NO_2 bond dissociation play important role among all of the initial channels for the p-nitrotoluene and m-nitrotoluene. For the o-nitrotoluene, the H atom migration and C-NO_2 bond dissociation are dominant reactions. In addition, there exist certain pathways for three isomers conversions, but with high energy barriers. Rate constant calculations and branching ratio analyses further demonstrate that the isomerization reactions of O transfer are prominent at low to intermediate temperature, whereas the direct C-NO_2 bond dissociation reactions prevail at high temperature for p-nitrotoluene and m-nitrotoluene. For o-nitrotoluene, H atom migration is predominant reaction. While C-NO_2 bond dissociation becomes important with the temperature increasing.

1. Introduction

Nitroaromatic compounds are important explosives which have wide ranges of military or industrial applications.[1-3] There has been an immense research interest in measuring the detonation characteristics[1-3] and sensitivities[4-7] of these kinds of compounds. These works refer that the initial chemical reactions including isomerization and decomposition are intimately connected to the explosive properties and sensitivities of nitroaromatic compounds, so that any approach giving access to detailed mechanisms of their initial reactions could provide significant improvement in understanding the explosive nature of nitroaromatic compounds.[8] However, previous evaluations of explosive and sensitivity properties were primarily based on empirical considerations.[9, 10] Moreover, due to the difficulties in experimental sampling, the experimental data are not always available or reliable.[11] Therefore, increasing works have been conducted to investigate the initial kinetics of nitroaromatic compounds. Cohen et al.[12] reported a comprehensive computational DFT investigation of the unimolecular adiabatic (thermal) decomposition of 2,4,6-tri-nitrotoluene (TNT), which still keeps the aromatic ring intact. Three possible pathways for TNT decomposition were postulated under different temperature conditions: (1) C-NO_2 homolysis, (2) isomerization of the nitro (NO_2) group to the nitrite (ONO), and (3) oxidation reactions of the methyl group. He et al.[13] revealed the shock decomposition process of 2,4,6-triamino-1,3,5-trinitrobenzene (TATB) by means of quantum-based multi-scale molecular dynamic calculations. Results show that the intermolecular hydrogen transfer becomes one of the most important reaction pathways for the initial decomposition of TATB. These works provide understanding of nitroaromatic compounds from a molecular point of view. Pitz et al.[14] developed a chemical kinetic model for gas phase combustion of TNT, which combines the data of decomposition and oxidation of TNT kinetics and the intermediate products in previous literature and from analogous reactions. However, there are major obstacles for developing kinetic mechanism for these kinds of explosives. For instance, the nitroaromatic compounds include more types of atoms than that are present in familiar hydrocarbons, including N atoms in the form of nitro groups. Typically, TNT and TATB have aromatic ring based structures with multiple substituted branches with N atoms. Despite those researches did on the thermal or shock decomposition of nitroaromatic explosives, there are still large voids of knowledge in the rates and mechanisms of specific reactions due to their chemical complexity.

Nitrotoluene, one of the simplest nitroaromatic compounds, is typically considered as model molecule to investigate their explosive properties.[15] It consists of three isomers: p-nitrotoluene, m-nitrotoluene and o-nitrotoluene. Several works have been carried out to characterize and rationalize the decomposition or isomerization mechanisms of nitrotoluene isomers through experiments and theoretical calculations of the initial reactions. The dissociation of the p-nitrotoluene molecular ion was investigated on a nanosecond time scale by using the photodissociation technique.[16] Results show that the experimental determined rate constant is in excellent agreement with the RRKM-QET calculation. However, there have no more detailed investigations on the reaction pathways and rate constants so far. In addition, the ultrafast dynamics of m-nitrotoluene and p-nitrotoluene radical cations were investigated with femtosecond pump-probe measurements and high-level DFT calculations by Boateng et al.[17]. Results show that coherent nuclear dynamics

a. State Key Laboratory of Multiphase Flow in Power Engineering, Xi'an Jiaotong University, Xi'an, 710049, People's Republic of China.
b. Department of Mechanical Engineering, The Hong Kong Polytechnic University, Hung Hom, Kowloon, Hong Kong
*Corresponding author: E-mail address: chenglongtang@mail.xjtu.edu.cn

contributions to C-NO$_2$ homolysis in both nitrotoluene radical cations and open up the potential for further investigation of coherent control schemes to manipulate dissociation pathways in nitroaromatic and other energetic molecules.

Tsang et al.[18] conducted the single pulse shock-tube decomposition investigations of o-nitrotoluene and p-nitrotoluene. They proposed that there are two important initial decomposition channels for p-nitrotoluene, C-NO$_2$ bond cleavage and C-NO$_2$ isomerization to form the nitrite prior to the breaking of the O-NO bond based on their experiments. However, for o-nitrotoluene there may remain another undefined primary channel to consume o-nitrotoluene due to thermally labile. Subsequently, He et al.[19] confirmed the undefined channel of o-nitrotoluene decomposition and deduced a mechanism through further experimental investigations, which is related to the intermediate: anthranil. Chen et al.[20] studied the kinetic mechanisms for the isomerization and decomposition of o-nitrotoluene in conjunction with rate constant predictions with RRKM and TST calculations. Results show that the channels producing CH$_3$C$_6$H$_4$ + NO$_2$, C$_6$H$_4$C(H)ON (anthranil) + H$_2$O, and CH$_3$C$_6$H$_4$O (o-methyl phenoxy) + NO are primary processes, whose high-pressure rate constants are 4.10 × 10^{17}exp[-37000/T] s^{-1}, 9.09 × 10^{12}exp[-25800/T] s^{-1} and 1.49 × 10^{14}exp[-30000/T] s^{-1}, respectively. Fayet et al.[8] investigated the influence of the substituent nature and position on the decomposition channels of o-nitrotoluene derivatives using the density function theory. They pointed out the complexity of the decomposition process in nitroaromatic compounds and suggested the C-NO$_2$ homolysis is not the predominant path for the studied o-nitrotoluene derivatives according to the related analysis of Gibbs activation energy. The multiple pathways for phototautomerization and energetic deactivation of o-nitrotoluene have been studied by Gudem and Hazra.[21] They suggest that a significant fraction of the isomerization yield is due to the triplet channel after considering the accessibility of different MECPs based on geometry and energy, and the magnitude of spin orbit coupling at singlet triplet MECPs. However, most of these works focused on the initial reactions of o-nitrotoluene, more detailed calculations of isomerization and decomposition of m-nitrotoluene and p-nitrotoluene such as the initial channels and mutual transformation among nitrotoluene isomers are necessary for understanding the kinetics of nitroaromatic compounds.

The motivation of this work arises from the growing interest in nitrotoluene isomers (p-, m- and o-nitrotoluene) as typical energetic model molecules and the need for development of the kinetic mechanisms about nitroaromatic compounds. Our objectives are the following. First of all, the detailed initial reaction pathways for each nitrotoluene isomer and the potential energy surfaces (PES) will be provided by highly accurate quantum calculation methods. In order to have a better understanding of the initial reaction process, rate constants will be calculated for dominant initial channels of each molecule. Since the rate constant calculation can shed further light on the competition mechanisms among different reaction pathways and provide valuable data for developing and improving combustion kinetic models of analogous systems, we then finally investigated the branching ratio of important initial reaction for each molecule to explore the importance of reaction at different temperature.

2. Computational Methods

2.1. Ab Initio Calculations

The initial reaction pathways of three nitrotoluene isomers (i.e., p-nitrotoluene, m-nitrotoluene and o-nitrotoluene) were firstly optimized by the B3LYP/6-311++G(d, p) method. The single-point energies were calculated by a coupled cluster theory with singles, doubles and perturbative inclusion of triples (CCSD(T)),[22, 23] with two large basis sets: the correlation-consistent, polarized-valence, double-ε (cc-pVDZ) and triple-ε (cc-pVTZ) basis set of Dunning.[24] The CCSD(T) energies were extrapolated to the complete basis set (CBS) limit via the following expression:

$$E_{SCF}^{(L)} = E_{SCF}^{(\infty)} + A exp(-\alpha\sqrt{X}) \quad (1)$$

where $E_{SCF}^{(L)}$ and $E_{SCF}^{(\infty)}$ are the self-consistent filed (SCF) energy with the highest angle quantum number L in basis set, and the energy of the CBS, respectively. In this study, L = 2 and 3 correspond to cc-pVDZ basis set and cc-pVTZ basis set, respectively; and α = 4.42.[25] Further, from the Eq. (1), the $E_{SCF}^{(\infty)}$ could be derived through

$$E_{SCF}^{(\infty)} = \frac{e^{\alpha\sqrt{3}}E_{SCF}^{(3)} - e^{\alpha\sqrt{2}}E_{SCF}^{(2)}}{e^{\alpha\sqrt{3}} - e^{\alpha\sqrt{2}}} \quad (2)$$

The zero-point energy corrections were obtained from the B3LYP/6-311++G(d, p) optimizations. This composite method has proved its validity and feasibility for many initial reactions of similar systems.[12, 20] Furthermore, the Q1 diagnostics have been performed for CCSD(T) calculations in order to assess the reliability of the single-reference correlation treatments,[26, 27] whose small Q1 values (smaller than 0.03) denotes the adequacy of CCSD(T) in the initial reaction processes of nitrotoluene isomers. The forward and reverse barrier heights are also calculated according to the reactant, TS and product energies including zero-point energy corrections. The forward barrier height is the difference between the TS and reactant energies; While the reverse barrier height is the difference between the TS and product energies. In addition, the intrinsic reaction coordinate (IRC) calculations were performed to confirm the connection between the designated transition states and the reactant or products. The Gaussian 09 program[28] was employed for all of the ab initio calculations.

2.2. Rate Constant Calculations

The rate constant of a reaction can be determined based on the potential energy surface (PES) of the reaction and properties of reactants, products and transition states including geometries, vibrational frequencies and rotational information. These properties were provided in the Supplementary material (see ESI†, Section S1). In addition, the thermochemical properties (enthalpies of formation at 298 K) of the reactants are necessary for the rate constant calculations and calculated as following[29]:

$$\Delta_f H^0(C_xH_yN_zO_n, 298\,K) = \Delta_f H^0(C_xH_yN_zO_n, 0\,K) +$$
$$[H^0(C_xH_yN_zO_n, 298\,K) - H^0(C_xH_yN_zO_n, 0\,K)] -$$
$$x[H^0(C, 298\,K) - H^0(C, 0\,K)]_{st} - y[H^0(H, 298\,K) -$$
$$H^0(H, 0\,K)]_{st} - z[H^0(N, 298\,K) - H^0(N, 0\,K)]_{st} -$$
$$n[H^0(O, 298\,K) - H^0(O, 0\,K)]_{st} \quad (3)$$

where $\Delta_f H^0(C_xH_yN_zO_n, 0\,K)$ is the theoretical enthalpies of formation at 0 K; $H^0(C_xH_yN_zO_n, 298\,K)$ and $H^0(C_xH_yN_zO_n, 0\,K)$ refer to the thermal correction to enthalpies and the zero-point

correction, respectively. Other items in Eq. (3) are the element enthalpy of formation corrections.

For theoretical enthalpies of formation at 0 K are performed by subtracting nonrelativistic atomization energies $\sum D_0$ from known enthalpies of all isolated atoms, as following the Eq. (4).

$$\Delta_f H^0\left(C_x H_y N_z O_n, 0\,K\right) = x\Delta_f H^0(C, 0\,K) + y\Delta_f H^0(H, 0\,K) + z\Delta_f H^0(N, 0\,K) + n\Delta_f H^0(O, 0\,K) - \sum D_0 \qquad (4)$$

Moreover, the nonrelativistic atomization energies were calculated by the Eq. (5)

$$\sum D_0 = xE(C) + yE(H) + zE(N) + nE(O) - ZPE \qquad (5)$$

where E and ZPE are the single-point energy and the zero-point energy, respectively.

The results have been provided in the Supplementary material (ESI,† Table S1). The temperature and pressure dependent rate constants of initial reaction channels for nitrotoluene isomers were calculated with the RRKM/Master Equation method.

Collision energy transfer is treated using an exponential-down model with $<\Delta E_{down}> = 150(T/300)^{0.85}$ cm^{-1}, which has been proved as a reasonable model by other literatures[30, 31]. The Lennard-Jones (L-J) pairwise potential is adopted to donate the interaction between reactant and bath gas (Ar is used in this work). The L-J parameters of Ar (σ = 3.465 Å, ε/k = 113.5 K) are taken from Mourits et al.[32]. For the nitrotoluene isomers, the L-J parameters are estimated by the empirical equations.[33]

$$\sigma = 2.44\ \left(T_c/P_c\right)^{1/3} \qquad (6)$$
$$\varepsilon_A/k_b = 0.77 T_c \qquad (7)$$

where k_b is the Boltzmann constant, T_c and P_c are the critical temperature and pressure, respectively. The method of Joback[34] is used to estimate the values of T_c and P_c for the initial reactants. These calculated results have been summarized in the Table 1.

Table 1. The Lennard-Jones (L-J) parameters for nitrotoluene isomers in this work.

Molecules	σ (Å)	ε_A/k_b (K)
R1	6.550	610.6
R2	6.370	529.3
R3	6.370	529.3
R4	6.438	601.8
R5	6.550	610.6
R6	6.370	529.3
R7	6.370	529.3
R8	6.438	601.8
R9	6.550	610.6
R10	6.370	529.3
R11	6.370	529.3
R12	5.610	509.6
R13	5.610	509.6
R14	5.610	509.6
R15	6.435	581.2

Tunneling effect has been demonstrated to be important at lower temperatures (500-1000 K) according to our previous work of nitrobenzene.[29] Thus, the one-dimensional approach, namely the unsymmetrical Eckart function,[35] is used in this work to consider the effect of tunneling. Specifically, the barrier width L is calculated through the following equations.

$$\frac{L}{2\pi} = \sqrt{-\frac{2}{F^*}\left[\frac{1}{\sqrt{E_1}} + \frac{1}{\sqrt{E_{-1}}}\right]^{-1}} \qquad (8)$$

$$v^* = \frac{1}{2\pi}\sqrt{-\frac{F^*}{m}} \qquad (9)$$

where F^* is the second derivative of the potential energy function evaluated at its maximum (force constant). E_1 and E_{-1} are the forward and reverse barrier heights at 0 K, respectively. v^* is the imaginary frequency of the transition state, and m is the reduced mass of the tunneling hydrogen. These values are also given in the Supplementary material (ESI,† Table S2).

3. Results and Discussion

### 3.1. Potential Energy Surface

Our calculations consider 29 initial reaction pathways of nitrotoluene isomers, including 15 isomerization reaction channels with energy barriers (transition states) and 14 direct bond dissociation channels. The optimized geometries of p-nitrotoluene, m-nitrotoluene and o-nitrotoluene, their isomers and transition states for the isomerization and dissociation products calculated at the B3LYP/6-311++G(d, p) level are presented in Figures 1-3. It is noted that reactant i is abbreviated as Ri, so throughout this paper, the reaction from Ri to Rj is abbreviated as Rxni-j, and the corresponding transition state is abbreviated as TSi-j. The p-nitrotoluene system includes R1-R4 isomers; The m-nitrotoluene system includes R5-R8 isomers; The o-nitrotoluene system includes R9-R15 isomers. In addition, for the p-nitrotoluene, m-nitrotoluene or o-nitrotoluene dissociated products we defined as the p-, m- or o-products, like the p-C$_6$H$_4$NO$_2$ representing the dissociated product of p-nitrotoluene.
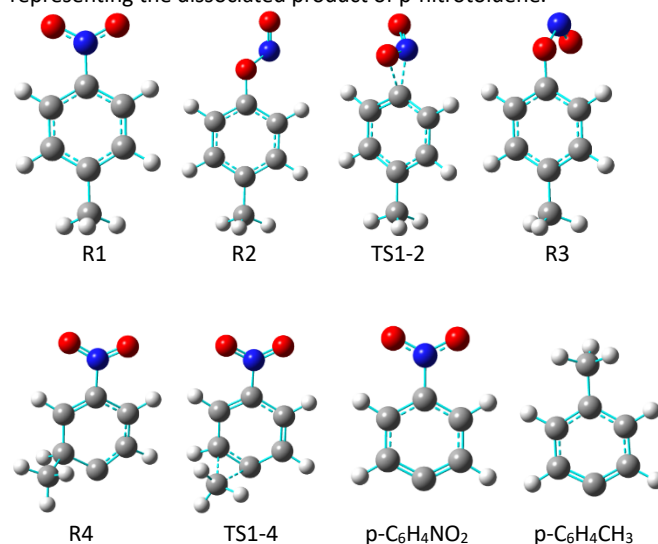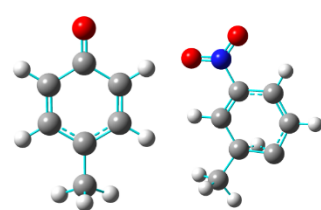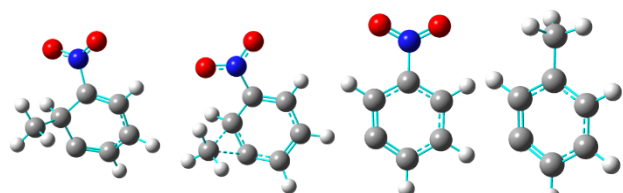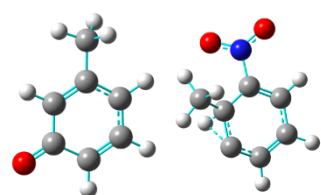
p-C$_6$H$_4$(O)CH$_3$ TS4-5

Figure 1. Optimized geometries of p-nitrotoluene, its isomers, transition states for the isomerization and dissociation products calculated at the B3LYP/6-311++G(d, p) level.
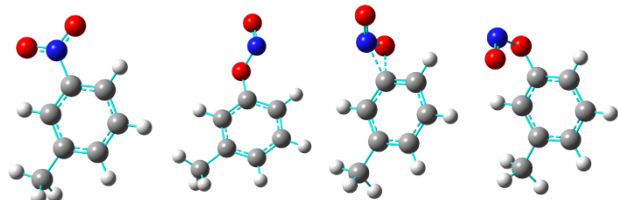
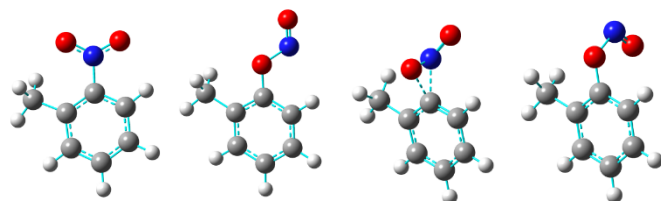R5   R6   TS5-6   R7
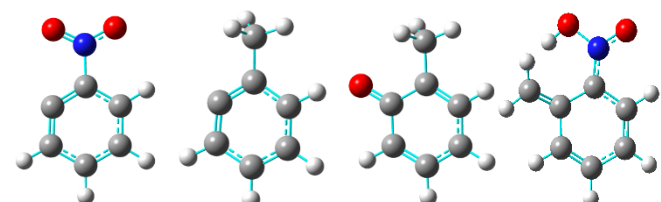

R8   TS5-8   m-C$_6$H$_4$NO$_2$ m-C$_6$H$_4$CH$_3$

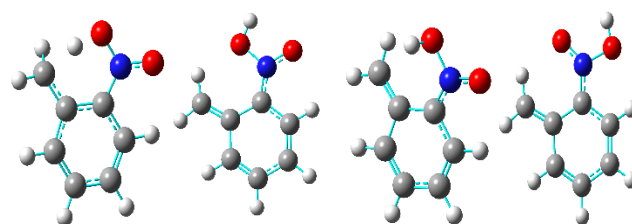m-C$_6$H$_4$(O)CH$_3$ TS8-9

Figure 2. Optimized geometries of m-nitrotoluene, its isomers, transition states for the isomerization and dissociation products calculated at the B3LYP/6-311++G(d, p) level.

R9   R10   TS9-10   R11

o-C$_6$H$_4$NO$_2$ o-C$_6$H$_4$CH$_3$ o-C$_6$H$_4$(O)CH$_3$ R12

TS9-12   R13   TS12-13   R14

TS13-14   R15   TS13-15   TS14-15

o- C$_6$H$_4$CH(O)N   o-C$_6$H$_4$CH$_2$NO

Figure 3. Optimized geometries of o-nitrotoluene, its isomers, transition states for the isomerization and dissociation products calculated at the B3LYP/6-311++G(d, p) level.
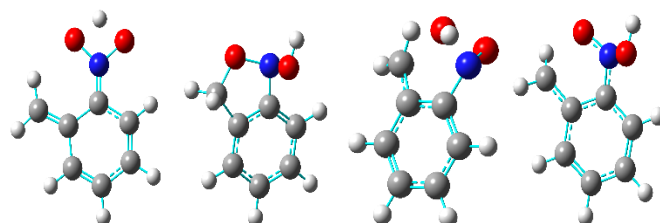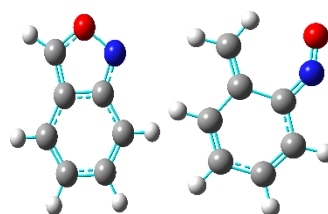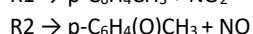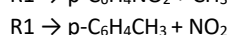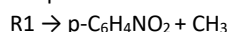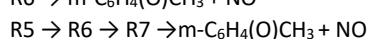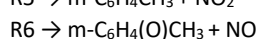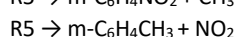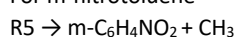
The conformational isomerism analyses of nitrotoluene isomers are conducted by scanning the rotation of single bonds at different positions with B3LYP/6-311++G(d, p) method and the calculated potential energy is shown in Figure 4. With torsion angle changing from 0° to 360°, three conformational isomerism processes are studied. It can be seen from Figure 4(a) that two energy minima (R2 and R3) are found with an energy difference of 1.8 kcal/mol. R2 and R3 have a similar optimized structure, in which only the nitro group has a different spatial position. The similar results are also observed in Figure 4(b) and 4(c). In addition, other important torsional models are also considered in calculations of the rate constants, which may be important at higher temperature.[36, 37]

The energy diagrams of the three nitrotoluene isomer systems including various isomerization and decomposition reactions optimized with the CCSD(T)/CBS method discussed above are shown in Figures 5-7. The major isomerization and decomposition channels of p-nitrotoluene, m-nitrotoluene and o-nitrotoluene consist of the following reactions:

For p-nitrotoluene
R1 → p-C$_6$H$_4$NO$_2$ + CH$_3$
R1 → p-C$_6$H$_4$CH$_3$ + NO$_2$
R2 → p-C$_6$H$_4$(O)CH$_3$ + NO
R1 → R2 → R3 → p-C$_6$H$_4$(O)CH$_3$ + NO
For m-nitrotoluene
R5 → m-C$_6$H$_4$NO$_2$ + CH$_3$
R5 → m-C$_6$H$_4$CH$_3$ + NO$_2$
R6 → m-C$_6$H$_4$(O)CH$_3$ + NO
R5 → R6 → R7 → m-C$_6$H$_4$(O)CH$_3$ + NO
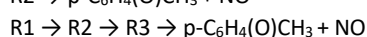
For o-nitrotoluene

R9 → o-$C_6H_4NO_2$ + CH_3

R9 → o-$C_6H_4CH_3$ + NO_2

R10 → o-$C_6H_4(O)CH_3$ + NO

R9 → R10 → R11 → o-$C_6H_4(O)CH_3$ + NO

R9 → R12 → R13 → R14 → R15 → o-$C_6H_4CH(O)N$ + H_2O

R9 → R12 → R13 → R15 → o-$C_6H_4CH(O)N$ + H_2O

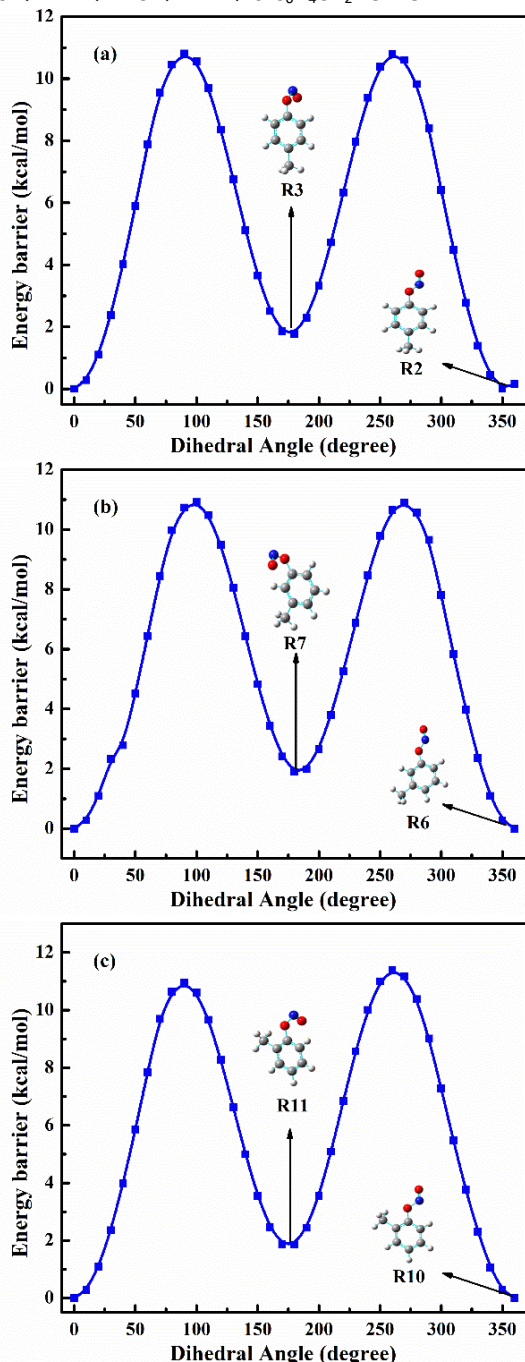R9 → R12 → R13 → R14 → o-$C_6H_4CH_2NO$ + OH

Figure 4. The rotational potential energies as a function of the torsion angle. The rotational potential energy surface of the O-N single bond from (a) R2, (b) R6, (c) R10, respectively.
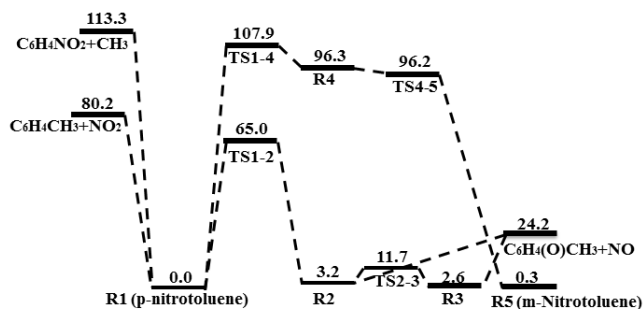

Figure 5. Calculated potential energy surfaces for major initial pathways of p-nitrotoluene at CCSD(T)/CBS level of theory.
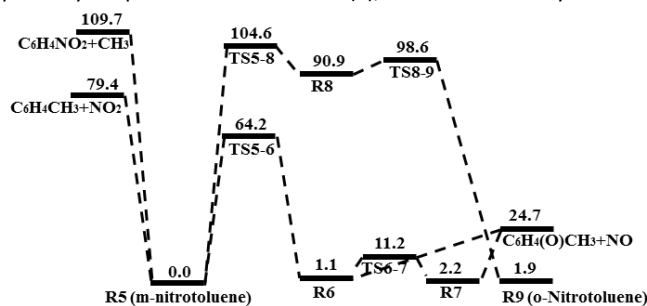

Figure 6. Calculated potential energy surfaces for major initial pathways of m-nitrotoluene at CCSD(T)/CBS level of theory.
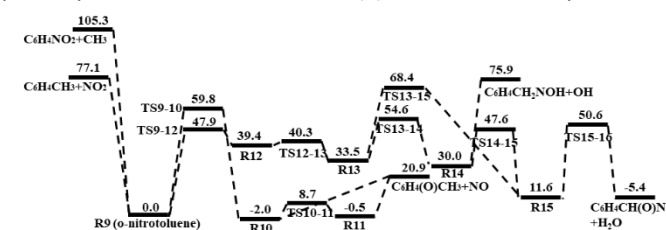

Figure 7. Calculated potential energy surfaces for major initial pathways of o-nitrotoluene at CCSD(T)/CBS level of theory.

In addition, the converted channels among three nitrotoluene isomers are also studied in this work. The characteristics of isomerization and decomposition reactions for the three nitrotoluene isomers will be discussed later.

3.1.1. Isomerization Reactions

For the main difference among the three studied nitrotoluene isomers is the position of CH_3 radical on the benzene ring, as shown in Figures 1-3 (the molecule structures of R1 (p-nitrotoluene) in Figure 1, R5 (m-nitrotoluene) in Figure 2 and R9 (o-nitrotoluene) in Figure 3). For p-nitrotoluene, the most important initial isomerization reaction chain is: R1 → R2 → R3. Specifically, the Rxn1-2 belongs to O transfer reaction, whose -NO_2 group changes from -NO_2 to -ONO. R1 isomerizes to R2 via TS1-2. R2 has a close stablity with R1, lying upon the R1 at 3.2 kcal/mol. The Rxn1-2 will accelerate the overall initial reaction process since it needs lower energy than R1 direct decomposition. There is a roaming-mediated isomerization like nitrobenzene isomerization process,[29] which is important for kinetic of nitrotoluene especially in low to intermediate temperature. R2 isomerizes to R3 with a barrier of 8.5 kcal/mol, which is conformational isomerization as discussed in Sec. 3.1. Whereas for m-nitrotoluene, the important initial isomerization reaction chain is: R5 → R6 → R7, which is similar to the p-nitrotoluene isomerization process. Rxn5-6 is also O transfer reaction, whose -NO_2 group changes from -NO_2 to -ONO. R5 needs 0.8 kcal/mol lower energy than

Rxn1-2. In addition, Rxn6-7 needs to go through TS6-7 of 10.1 kcal/mol, 1.6 kcal/mol higher than Rxn2-3. Fox o-nitrotoluene, it is well known that there are two important pathways: O atom migration and H atom migration [15, 38]. The key initial isomerization reaction chain is: R9 → R10 → R11. We also note that the calculated energy barrier of Rxn9-10 agrees well with that calculated in Chen et al.[20]. In addtion, the H atom migration channel from R9 to R12 only needs 47.9 kcal/mol, which is 10.9 kcal/mol lower than Rxn9-10. The H atom migration channel can only occur in the o-nitrotoluene system, since it has a very close distance between –CH_3 group and –NO_2 group.

The three isomers can also be transformed through muti-step isomerization reactions: R1 (p-nitrotoluene) → R4 → R5 (m-nitrotoluene) → R8 → R9 (o-nitrotoluene). It can be seen that p-nitrotoluene can isomerize to m-nitrotoluene through Rxn1-4 and Rxn4-5. First, R1 needs to go through TS1-4 of 107.9 kcal/mol to generate R4, which is unstable structure, then isomerize to R5 through TS4-5. This process includes positions exchange between the para-position CH_3 radical and the meta-position H radical. Then CH_3 radical on R5 transfers to the ortho-position C atom to generate R8, which goes through 104.6 kcal/mol energy barriers. Finanlly, R8 isomerizes to R9 through the ortho-position H radical transfering to the meta-position C atom. It is note that the p-nitrotoluene and o-nitrotoluene can not be converted into each other directly due to very high energy barrier.

3.1.2. Decomposition Reactions

With regard to each nitrotoluene isomer (p-, m- or o-nitrotoluene), there are four accessible decomposition pathways, including two direct bond dissociation channels of R1, R5 or R9, as shown in Figures 5-7. The bond dissociation energies of the C-N bonds for p-, m- and o-nitrotoluene at the CCSD(T)/CBS//B3LYP/6-311++G(d, p) level are 80.2 kcal/mol, 79.4 kcal/mol and 77.1 kacl/mol, respectively. These energy levels agree well with the experimental results from Pruitt and Goebbert.[39] In their work, the dissociation energy of p-nitrotoluene is 78.2 ± 5.1 kcal/mol, m-nitrotoluene is 75.9 ± 4.4 kcal/mol, and o-nitrotoluene is 75.2 ± 3.9 kcal/mol. The calculated dissociation energies for the three isomers of nitrotoluene as well the experimetal results from literature indicate that the CH_3 substitution and its position on the aromatic ring have influence on the energy of the C-N bond. Especically, for p-nitrotoluene, the dissociation energy is obvious higher than m- and o-nitrotoluene. When CH_3 radical position closes to C-NO_2 bond, the C-N bond dissociation energy becomes low. The reason may be that the CH_3 radical changes the C-C bond of aromatic ring, which makes the C-N bond energy change accordingly. For the bond dissociation energies of C-CH_3 bonds for p-, m- and o-nitrotoluene are 113.3 kcal/mol, 109.7 kcal/mol and 105.3 kcal/mol, respectively. Chen et al.[20] showed that the o-nitrotoluene molecule dissociates directly to the products $C_6H_4CH_3$ + NO_2 with the dissociation energy of 76.3 kcal/mol and to $C_6H_4NO_2$ + CH_3 with the high dissociation energy of 103.0 kcal/mol. Their calculated results also agree with the results in this work. The dissociation energy of p-nitrotoluene is larger than the other two isomers; m-nitrotoluene has relatively larger dissociation energy than o-nitrotoluene. Therefore, from above discussions on the two direct decomposition reactions for three nitrotoluene isomers, it can be concluded that the -CH_3 group and -NO_2 group have a mutual influence. When their positions

are close, dissociation of the C-CH_3 bond or C-NO_2 bond happens easily.

The other decomposition pathways of the three isomers are the $C_6H_5CH_3$-ONO and its conformational isomer dissociation reaction to form $C_6H_5CH_3O$ + NO. The bond dissociation energies of R2, R6 and R10 are 21.2 kcal/mol, 23.6 kcal/mol and 22.9 kcal/mol, respectively. While the bond dissociation energies of R3, R7 and R11 are 21.6 kcal/mol, 22.1 kcal/mol and 21.5 kcal/mol, respectively. It can be seen that there are no obvious difference about bond dissociation energy of O-NO. The O-NO bond dissociation energy is lower than the corresponding isomer direct bond dissociation energy. However, the O-NO bond dissociation process needs to go through the O transfer isomerization reaction first, and then the activity of O-NO bond dissociation is greatly reduced. In addition, according to the experiments of o-nitrotoluene from Schmierer et al.[15] and Boateng et al.[38], the decomposition channels which can generate H_2O or OH have great influence on o-nitrotoluene initial consumption. Therefore, the corresponding channels have been studied. It can be seen that the main decomposition channels are: R9 → R12 → R13 → R14 → R15 → o-$C_6H_4CH(O)N$ + H_2O, R9 → R12 → R13 → R15 → o-$C_6H_4CH(O)N$ + H_2O and R9 → R12 → R13 → R14 → o-$C_6H_4CH_2NO$ + OH. The R15, which can be obtained from R13 and R14 via TS13-15 and TS14-15, respectively, can eliminate H_2O to give the double-ring product o-$C_6H_4CH(O)N$ by overcoming 39.0 kcal/mol barrier. During the dehydration process, the R14 can also decompose to OH radical. However, these processes are all need go through mutil-step reactions to decompose.

3.2. Calculated Rate Constants

For the three nitrotoluene isomer molecules, only the prodominant pathways disscussed above, i.e., the isomerization and direct bond dissociation reactions, are taken into consideration for the rate constant calculations. The isomerization channels consist of channels (Rxn1-2, Rxn2-3, Rxn1-4 and Rxn4-5) for p-nitrotoluene, channels (Rxn5-6, Rxn6-7, Rxn5-8 and Rxn8-9) for m-nitrotoluene, channels (Rxn9-10, Rxn10-11, Rxn9-12, Rxn12-13, Rxn13-14, Rxn14-15 and Rxn13-15) for o-nitrotoluene. The direct bond dissociation channels consist of channels from R1, R2 and R3 for p-nitrotoluene, channels from R5, R6 and R7 for m-nitrotoluene, and channels from R9, R10, R11, R14 and R15 for o-nitrotoluene. In addition, calculated rate constants at high pressure limit in the temperature range of 500-2000 K for different channels were fitted to the quasi-Arrhenius correlation, as in Table 2. These parameters can be directly used in combustion modeling. The corresponding activation energies of barrier isomerization reaction (E_a in the quasi-Arrhenius correlation, kcal/mol) provided in the figure as well as in Table 2 are fitted. It can also reflect the energy barrier of the reaction.

Calculated rate constants at high pressure limit have been plotted in Figure 8 for p-nitrotoluene, Figure 9 for m-nitrotoluene and Figure 10 for o-nitrotoluene. With p-nitrotoluene, the channels depicted in Figure 6 include four isomerization channels and four direct bond dissociation channels. From Figure 8, rate constants of all the eight channels increase with the increase of temperature. For reactions in which R1 is the direct reactant, the Rxn1-2 and reaction: R1 → $C_6H_4CH_3$ + NO_2 have relatively high rate constants. While, the Rxn1-4 and reaction: R1 → $C_6H_4NO_2$ + CH_3 have low reactivities at the whole temperature range. It also indicates that the C-NO_2 bond

dissociation is much easier than the C-CH$_3$ bond dissociation at the same temperature. For the converted channels (R1 → R4 → R5) between p-nitrotoluene and m-nitrotoluene, the Rxn4-5 has the highest rate constant among eight studied reactions. However, rate constant of Rxn1-4 is the lowest. We can also find that the activation energy of Rxn1-4 (137.7 kcal/mol) is much higher than that of Rxn4-5 (0.3 kcal/mol). Therefore, p-nitrotoluene is very difficult to isomerize to m-nitrotoluene. For the direct bond dissociation of R2 and R3, these two reactions have very close rate constant and are higher than the rate constant of R1 → C$_6$H$_4$CH$_3$ + NO$_2$ under low to intermedicate temperature. In addition, the rate constant of conformational isomerism channel between R2 and R3 is very high, which means Rxn2-3 can happen easily. For the dissociation of R2 and R3, they need first to be isomerized from p-nitrotoluene. Among the multiple-step channels, the TS12 with a 65.0 kcal/mol barrier is the primary rate-controlling step.

Table 2. Rate constants for nitrotoluene initial reactions with quasi-Arrhenius form[a] at high pressure limit.

Type	Reaction	log$A$	E_a	n
p-nitrotoluene	Rxn1-2	13.0	63.5	0.3
	Rxn2-3	11.7	7.8	0.5
	Rxn1-4	79.9	137.7	-20.1
	Rxn4-5	11.1	0.3	0.5
	R1 → C$_6$H$_4$NO$_2$ + CH$_3$	24.2	102.3	-1.7
	R1 → C$_6$H$_4$CH$_3$ + NO$_2$	25.8	81.0	-2.2
	R2 → C$_6$H$_4$(O)CH$_3$ + NO	21.2	34.3	-3.4
	R3 → C$_6$H$_4$(O)CH$_3$ + NO	22.1	35.3	-3.8
m-nitrotoluene	Rxn5-6	12.6	62.3	0.4
	Rxn6-7	11.7	9.5	0.5
	Rxn5-8	11.5	102.8	0.4
	Rxn8-9	12.6	6.4	0.1
	R5 → C$_6$H$_4$NO$_2$ + CH$_3$	24.3	113.54	-4.2
	R5 → C$_6$H$_4$CH$_3$ + NO$_2$	25.7	88.0	-2.1
	R6 → C$_6$H$_4$(O)CH$_3$ + NO	20.7	37.5	-3.4
	R7 → C$_6$H$_4$(O)CH$_3$ + NO	21.1	36.5	-3.7
o-nitrotoluene	Rxn9-10	13.4	57.2	0.2
	Rxn10-11	11.6	10.1	0.5
	R9 → C$_6$H$_4$NO$_2$ + CH$_3$	22.7	106.9	-1.0
	R9 → C$_6$H$_4$CH$_3$ + NO$_2$	24.0	85.6	-1.4
	R10 → C$_6$H$_4$(O)CH$_3$ + NO	21.0	36.2	-3.4
	R11 → C$_6$H$_4$(O)CH$_3$ + NO	22.2	35.2	-3.8
	Rxn9-12	11.2	43.6	1.3
	Rxn12-13	13.1	1.2	0.05
	Rxn13-14	11.8	17.9	0.3
	Rxn13-15	12.0	33.4	0.3
	Rxn14-15	12.1	17.0	0.1
	R15 → C$_6$H$_4$C(H)ON + H$_2$O	12.2	36.3	0.5
	R14 → C$_6$H$_4$CH$_2$NO + OH	7.2	44.0	1

[a] $k = AT^n \exp(-E_a/RT)$; units: k: s^{-1}, E_a: kcal/mol, T: K.
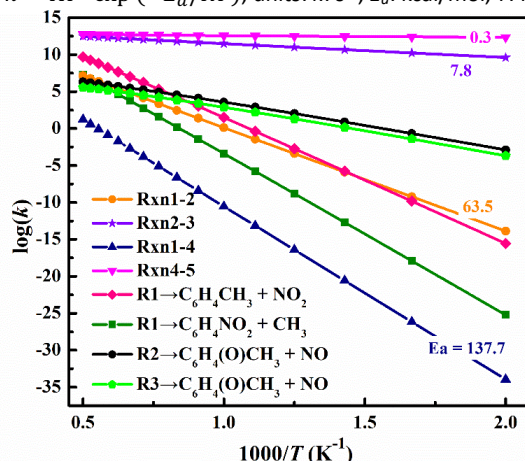

Figure 8. Calculated rate constants at high pressure limit for major channels of p-nitrotoluene initial reactions at the temperature range of 500-2000 K.

Figure 9 shows the rate constants at different temperatures for m-nitrotoluene initial reactions. Similar to p-nitrotoluene, rate constants of the eight channels increase with temperature. For the four bond dissociation channels, the rate constant of the reaction R5 decomposition to CH$_3$ radical is the lowest, which indicates this channel can hardly happen. The rate constants of conformational isomers (R6 and R7) dissociation are larger than that of R5 → C$_6$H$_4$CH$_3$ + NO$_2$ at T < 1200 K, whereas the rate constant of R5 → C$_6$H$_4$CH$_3$ + NO$_2$ becomes larger at T > 1200 K. The m-nitrotoluene (R5) can isomerize to o-nitrotoluene (R9) through R5 → R8 → R9 channel, but it needs to go through 102.8 kcal/mol and 6.4 kcal/mol energy barrier, respectively according to the calculated rate constants. For the isomerization channel of Rxn5-6, it has a competition with the bond dissociation of R5 → C$_6$H$_4$CH$_3$ + NO$_2$. When T > 1000 K, the C-NO$_2$ bond dissociation rate constant is larger than the rate constant of Rxn5-6. However, the rate constant of Rxn5-6 is larger than that of R5 → C$_6$H$_4$CH$_3$ + NO$_2$ at T < 1000 K.
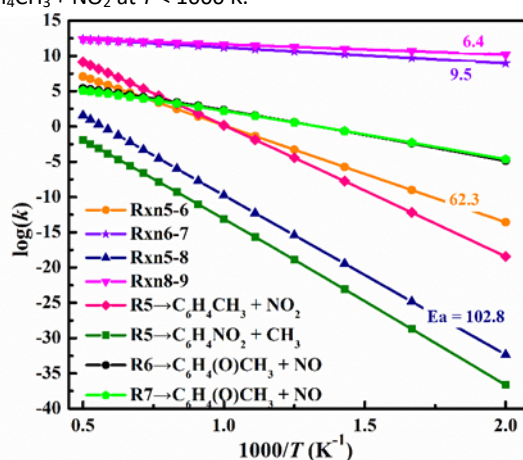

Figure 9. Calculated rate constants at high pressure limit for major channels of m-nitrotoluene initial reactions at the temperature range

of 500-2000 K.

Figure 10 plots the rate constants of channels for o-nitrotoluene. Rate constant computations have been conducted for 13 channels, including 7 isomerization channels and 6 direct bond dissociation channels. It is note that there have no channels to make the o-nitrotoluene isomerize to p-nitrotoluene. The rate constant of Rxn12-13 is the largest among calculated channels of o-nitrotoluene. The Rxn9-10 has larger rate constant than R9 → $C_6H_4CH_3$ + NO_2 at low temperature (T < 1050 K), and has smaller rate constant than R9 → $C_6H_4CH_3$ + NO_2 at high temperature (T > 1050 K). However, the Rxn9-12 has the largest rate constant among the Rxn9-10, R9 → $C_6H_4CH_3$ + NO_2 and R9 → $C_6H_4NO_2$ + CH_3. It indicates that the o-nitrotoluene is difficult to decompose to CH_3 radical. Due to the CH_3 group is adjacent to the NO_2 group, there are special channels for o-nitrotoluene. The reactions of decomposing to H_2O or OH also play a very important role in o-nitrotoluene initial reactions. In addition, the conformational isomers (R10 and R11) of o-nitrotoluene have very colse rate constant, similar with the p-nitrotoluene and m-nitrotoluene cases.
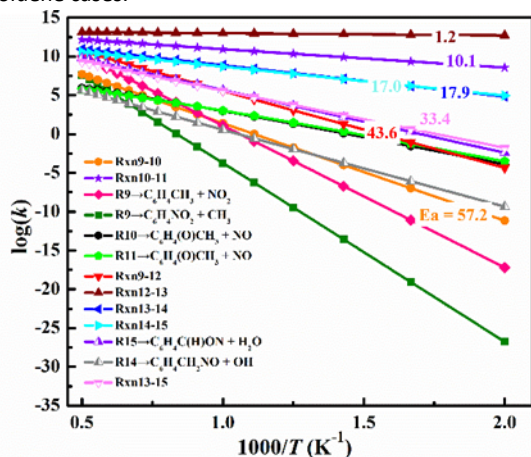

Figure 10. Calculated rate constants at high pressure limit for major channels of o-nitrotoluene initial reactions at the temperature range of 500-2000 K.

For the bond dissociation reaction of o-nitrotoluene (R9 → $C_6H_4CH_3$ + NO_2 in this work), many researchers have done investigations both numerically and experimentally. Figure 11 shows the calculated rate constants of R9 → $C_6H_4CH_3$ + NO_2 from this paper and Chen et al.[20], as well as the experimental data from Ref. 40, Ref. 18 and Ref. 19, at temperature range from 950 K to 1300 K. It can be seen that the rate constants measured by Gonzalez et al.[40] using the SF_6 as bath gas at 110 Torr pressure are evidently higher than those measured by Tsang and co-workers[18, 19] using Ar as bath gas at 2700-3400 Torr. The calculated rate constant from Chen et al. agrees closely with the experimental data from Gonzalez et al., while is slightly higher than those measured data by Tsang and co-workers. The rate constant calculated in this paper shows relatively better agreement with these experimental data in Figure 11.
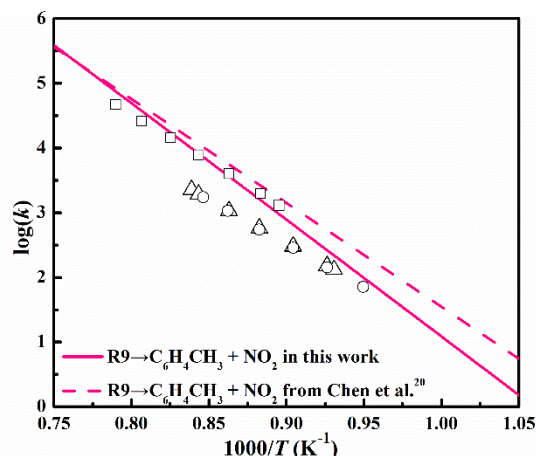

Figure 11. Predicted rate constants for R9 → $C_6H_4CH_3$ + NO_2 (solid line: this work; dash line: Chen et al.[20]). Experimental data: □ Ref. 40, △ Ref. 18, ○ Ref. 19.

3.3. Comparison of Rate Constants of p-, m- and o-nitrotoluene Isomerization and Direct Decomposition Channels

To compare the importance of these initial channels, we provid the high pressure limit branching ratios of the key decomposition channels, together with the isomerization reactions which are directly related to p-, m- and o-nitrotoluene in Figure 12 for the temperature range of 500–2000K. Figure 12(a) shows the initial channel branching ratios of p-nitrotoluene. It can be seen that the branching ratios of Rxn1-4 and R1 → $C_6H_4NO_2$ + CH_3 are negligibly small for the whole temperature range. When the temperature is higher than around 1050 K, the decomposition through C-NO_2 bond break dominates the initial reaction of p-nitrotoluene. In addition, the isomerization reaction Rxn1-2 becomes dominant among all the isomerization reactions as well as the decomposition reactions as temperature decreases to below 1050 K. At this temperature range, Rxn1-2 has a branching ratio of more than 0.5, and its importance becomes even more significant at lower temperature. In this work, we have also considered the possibility that nitrotoluene can directly decompose to NO. However, it is found that this channel is very unlikely to occur. The NO radical can be generated through the channel of R1 → R2 or R1 → R2 → R3, like our previous work of nitrobenzene. Because reactions R2 → p-C_6H_4(O)CH_3 + NO and R2 → R3 → p-C_6H_4(O)CH_3 + NO have high rate constants, they are important reactions at p-nitrotoluene initial process, especially at low to intermediate temperature. For m-nitrotoluene, similar conditions can be found in Figure 12(b). The branching ratios of isomerization reaction Rxn5-8 and C-CH_3 bond dissociation reaction of R5 are negligibly small at 500-2000 K. When T is higher than 1000 K, the C-NO_2 bond dissociation of m-nitrotoluene is predominant. While the isomerization reaction Rxn5-6 becomes predominant at T < 1000 K. For the o-nitrotoluene system, the branching ratio of R9 → $C_6H_4NO_2$ + CH_3 can be negligible. The Rxn9-12 dominants the initial reactions of o-nitrotoluene. While with the temperature increase, the importance of R9 → $C_6H_4CH_3$ + NO_2 increases.
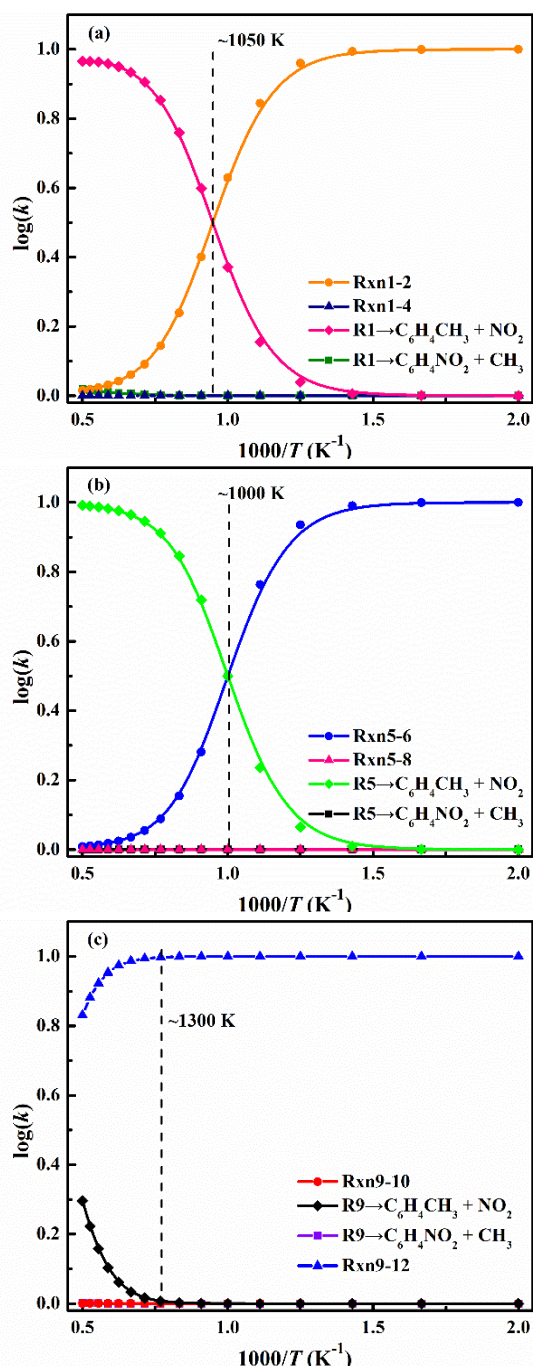
Figure 12. Calculated branching ratios for the direct decomposition reactions and isomerization reactions at high pressure limit in the temperature range 500–2000 K for (a): p-nitrotoluene; (b): m-nitrotoluene and (c): o-nitrotoluene.

4. Conclusions

The initial reaction mechanisms for three nitrotoluene molecules p-nitrotoluene, m-nitrotoluene and o-nitrotoluene, have been investigated theoretically by using the ab initio approach. The PESs of all molecules studied in this paper have been constructed with the CCSD (T)/CBS//B3LYP/6-311++G(d, p) method. For the p-nitrotoluene and o-nitrotoluene, the C-NO$_2$ bond breaking and C-NO$_2$ transfering to -ONO isomerization reactions are predicted to be the most

important processes in their initial reactions. While for the o-nitrotoluene, the H atom migration and the C-NO$_2$ bond breaking dominate the inition reactions. The three isomes can be converted through the channel of R1 (p-nitrotoluene) $\rightarrow$ R4 $\rightarrow$ R5 (m-nitrotoluene) $\rightarrow$ R8 $\rightarrow$ R9 (o-nitrotoluene), but it needs to go through very high energy barrier to be active. Further rate constant calculations and branching ratio analyses indicate that for the p-nitrotoluene and m-nitrotoluene, the isomerization reactions of C-NO$_2$ group are predominant at low to intermediate temperature (about T < 1000 K), wheresa the direct C-NO$_2$ bond dissociation reactions are dominant at high temperature (about T > 1000 K). For o-nitrotoluene, the Rxn9-12 are dominant at the whole temperature range, while with the temperature increse the C-NO$_2$ bond dissociation become important. Calculated rate constants at high pressure limit at 500-2000 K for different channels were fitted to the modified Arrhenius equations, which can be used directly in combustion mechanism construction of nitroaromatic compounds (like TNT) combustion in the future.

Conflicts of Interest

There are no conflicts of interest to declare.

Acknowledgments

Notes and references

1.   M. H. Keshavarz, *Propell. Explos. Pyrot.*, 2012, **37**, 93-99.
2.   M. H. Keshavarz, H. R. Pouretedal, H. Sadeghi and A. Semnani, *Propell. Explos. Pyrot.*, 2010, **34**, 415-420.
3.   G. Fayet and P. Rotureau, *Phys. Chem. Chem. Phys.*, 2010, **16**, 6614-6622.
4.   P. E. Shaw, H. Cavaye, S. S. Y. Chen, M. James, I. R. Gentle and P. L. M. Burn, *Phys. Chem. Chem. Phys.*, 2013, **15**, 9845-9853.
5.   M. H. Keshavarz, *J. Hazard. Mater.*, 2008, **153**, 201-206.
6.   P. Politzer and J. S. Murray, *J. Mol. Model.*, 2015, **21**, 25.
7.   T. L. Jensen, J. F. Moxnes, E. Unneberg and D. Christensen, *J. Mol. Model.*, 2020, **26**, 65.
8.   G. Fayet, L. Joubert, P. Rotureau and C. Adamo, *J. Phys. Chem. A*, 2009, **113**, 13621-13627.
9.   M. H. Keshavarz, *J. Hazard. Mater.*, 2007, **145**, 263-269.
10.   T. Grewer, *Thermochim. Acta*, 1991, **187**, 133-149.
11.   R. J. A. Kersten, M. N. Boers, M. M. Stork and C. Visser, *J. Loss Prevent. Proc.*, 2005, **18**, 145-151.
12.   R. Cohen, Y. Zeiri, E. Wurzberg and R. Kosloff, *J. Phys. Chem. A*, 2007, **111**, 11074.
13.   Z. H. He, J. Chen and Q. Wu, *J. Phys. Chem. C*, 2017, **121**, 8227-8235.
14.   W. J. Pitz and C. K. Westbrook, *Proc. Combust. Inst.*, 2007, **31**, 2343-2351.

15. T. Schmierer, S. Laimgruber, K. Haiser, K. Kiewisch, J. Neugebauer and P. Gilch, *Phys. Chem. Chem. Phys.*, 2010, **12**, 15653-15664.

16. J. C. Choe and M. S. Kim, *J. Phys. Chem. B*, 1991, **95**, 50-56.

17. D. A. Boateng, G. L. Gutsev, P. Jena and K. M. Tibbetts, *J. Chem. Phys.*, 2018, **148**, 134305.

18. W. Tsang, D. Robaugh and W. G. Mallard, *J. Phys. Chem.*, 1986, **90**, 5968-5973.

19. Y. Z. He, J. P. Cui, W. G. Mallard and W. Tsang, *J. Am. Chem. Soc.*, 1988, **110**, 3754-3759.

20. S. C. Chen, S. C. Xu, E. Diau and M. C. Lin, *J. Phys. Chem. A*, 2006, **110**, 10130-10134.

21. M. Gudem and A. Hazra, *J. Phys. Chem. A*, 2018, **122**, 4845-4853.

22. K. Raghavachari, G. W. Trucks, J. A. Pople and M. Head-Gordon, *Chem. Phys. Lett.*, 1989, **157**, 479-483.

23. H. Koch, O. Christiansen, R. Kobayashi, P. J. Rgensen and T. Helgaker, *Chem. Phys. Lett.*, 1994, **228**, 233-238.

24. A. W. Jasper, S. J. Klippenstein, L. B. Harding and B. Ruscic, *J. Phys. Chem. A*, 2007, **111**, 3932-3950.

25. F. Neese, The ORCA program system. Wiley Interdip. Rev. Comput. Mol. Sci. 2012, **2**, pp: 73-78.

26. T. J. Lee, A. P. Rendell and P. R. Taylor, *J. Chem. Phys.*, 1990, **92**, 489-495.

27. T. J. Lee and P. R. Taylor, *Int. J. Quantum Chem.*, 1989, **36**, 199-207.

28. M. J. Frisch, G. W. Trucks, H. B. Schlegel, G. E. Scuseria, M. A. Robb, J. R. Cheeseman, G. Scalmani, V. Barone, B. Mennucci, G. A. Petersson, H. Nakatsuji, M. Caricato, X. Li, H. P. Hratchian, A. F. Izmaylov, J. Bloino, G. Zheng, J. L. Sonnenberg, M. Hada, M. Ehara, K. Toyota, R. Fukuda, J. Hasegawa, M. Ishida and T. Nakajima, Gaussian 09, Gaussian Inc, Wallingford CT, 2009.

29. Z. Q. Gao, M. Yang, C. L. Tang, F. Y. Yang, X. S. Fan, R. Yang and Z. H. Huang, *Chem. Phys. Lett.*, 2019, **715**, 244-251.

30. E. E. Greenwald, S. W. North, Y. Georgievskii and S. J. Klippenstein, *J. Phys. Chem. A*, 2005, **109**, 6031-6044.

31. R. Sivaramakrishnan, M. C. Su, J. V. Michael, S. J. Klippenstein and B. Ruscic, *J. Phys. Chem. A*, 2011, **115**, 3366-3379.

32. F. M. Mourits and F. H. A. Rummens, *Canad. J. Chem.*, 1977, **55**, 3007-3020.

33. J. R. Welty, C. E. Wicks, R. E. Wilson and G. L. Rorrer, Fundamentals of momentum, heat and mass transfer, 4th ed.; John Wiley and Sons Ltd.: New York, 2001.

34. Cox, K.cR.; Chapman, W. G. The Properties of Gases and Liquids, fifth ed., 2001.

35. H. S. Johnston and J. Heicklen, *J. Phys. Chem.*, 1962, **66**, 532-533.

36. J. J. Zheng, R. M. Pañeda and D. G. Truhlar, *J. Am. Chem. Soc.* 2014, **136**, 5150-5160.

37. J. L. Bao and D. G. Truhlar, *Chem. Soc. Rev.*, 2017, **46**, 7548-7596.

38. D. A. Boateng, M. K. D. Word, L. G. Gutsev, P. Jena and K. M. Tibbetts, *J. Phys. Chem. A*, 2019, **123**, 1140-1152.

39. C. J. M. Pruitt and, D.J. Goebbert, *Chem. Phys. Lett.*, 2013, **580**, 21-27.

40. A. C. Gonzalez, C. W. Larson, D. F. Mcmillen and D. M. Golden, *J. Phys. Chem.*, 1985, **89**, 4809-4814.